Microvariability of Line Profiles in the Spectrum of the Star ι Her

A. F. Kholtygin[1], G. A. Galazutdinov[2,3], T. E. Burlakova[2,4], G. G. Valyavin[2,4], S. N. Fabrika[2], and B.-C. Lee[4]

[1] *Astronomical Institute, St. Petersburg State University, Universitetskii pr. 28, Petrodvorets, 198504 Russia*

[2] *Special Astrophysical Observatory, Russian Academy of Sciences, Nizhniĭ Arkhyz, Karachaĭ-Cherkessian Republic, 357147 Russia*

[3] *Korea Astronomy and Space Science Institute, 61-1, Hwaam-dong, Yuseong-gu, Daejeon, 305-348 Republic of Korea*

[4] *Bohynsan Optical Astronomy Observatory, Jacheon P.O.B., Young-chun, Kyung-pook, 770-820 Republic of Korea*

Received April 7, 2005; in final form, September 7, 2005

Abstract—We present the results of a search for and analysis of line-profile variations in the spectrum of the star ι Her. The observations were acquired with the 1.8 m telescope of the Bohyunsan Optical Astronomy Observatory (Republic of Korea) in May–June 2004. We obtained 69 spectra of the star with signal-to-noise ratios ≈300 and a time resolution of 5–7 min. Profile variability was revealed for six lines of HI, HeI, and SiIII, in the central parts of the lines. The variability amplitude is ≈$(1-2)$% in units of the intensity of the adjacent continuum. Evidence was found for cyclic variations of the lines, with periods from ≈$7^{\rm h}$ to ≈$2.9^{\rm d}$. We conclude that ι Her belongs to the group of slowly pulsating stars.

1. INTRODUCTION

Variable stars on the upper main sequence can be divided into two large groups: β Cephei stars and slowly pulsating B stars (SPB stars), which have been suggested as a special group of variable stars in [1]. SPB stars have the spectral types B2–B5 and exhibit multiperiodic photometric variations on time scales from several hours to ≈2 days. These variations are usually interpreted as high-order g modes of nonradial pulsations (NRPs) (cf., for instance, [2]). Of special interest is the stellar subgroup in the intermediate region of the Hertzsprung–Russell (HR) diagram, between the β Cep and SPB stars. It is supposed that these stars have features of both stellar groups.

One of the most interesting members of this subgroup is the bright B3IV–V star ι Her (85 Her, HR 6588, HD 160762, $V = 3.80^m$).

Over more than 80 years of studies of ι Her, several dozen periods for the regular spectral and photometric variations have been found, ranging from ≈$1^{\rm h}$ to $113^{\rm d}$. Variations of the MgII 4481 Å and HeI 4388 Å line profiles in the stellar spectrum on time scales of $0.14^{\rm d}$ were already detected in the early study [3]. It was established in [4, 5] that ι Her was a spectroscopic binary with an orbital period of $113^{\rm d}$ and a low-mass ($M \leq 0.4\,M_\odot$) companion.

The detection of line-profile variations with periods between $10^{\rm h}$ and $14^{\rm h}$, interpreted as NRP g modes, was reported in [6]. Smith [7] observed short-period profile variations of weak lines in the spectrum of ι Her on time scales of ≈$2^{\rm h}$. Chapellier *et al.* [8] detected V brightness variations with an amplitude of ≈0.01^m and periods of $0.12^{\rm d}$ and $0.14^{\rm d}$. The same periods were derived for radial-velocity variations of ι Her measured for lines at $\lambda\lambda\,3850-4750$ Å.

The most complete photometric and spectroscopic study of the ι Her systm is that of Chapellier *et al.* [9], who analyzed their own photometric and spectroscopic observations acquired during the decade following 1985, together with Hipparcos photometric measurements (1990–1993) [10] and all earlier published radial-velocity measurements. Despite the very large data volume used, they were able to reliably detect only one regular component, with the frequency $\nu_1 = 0.28671$ d^{-1}. The possible presence of radial-velocity variations with frequencies of 0.43, 0.77, and 0.2483 d^{-1} was noted.

The very large number of periods for the regular brightness and radial-velocity variations detected for ι Her suggests that far from all of the inferred variations are real, and that some could have arisen due to errors in data reduction, as well as to the superposition and interference of different regular components. It is also possible that the variations have a transient character, so that they may exist at one epoch and disappear or become irregular at another.

In order to better understand the nature of ι Her and to find which of the frequencies for the star's photometric and spectroscopic variations were real, we acquired observations of ι Her with high spectroscopic and time resolution in May−June 2004 with the 1.8 m telescope of the Bohyunsan Optical Astronomy Observatory (BOAO) in South Korea.

We present the main characteristics of the ι Her system in Section 2. The observations and a description of our reduction of the spectrograms are presented in Section 3. Section 4 describes the general pattern of the line-profile variations on various time scales. The results of our Fourier analysis of the line-profile variations are presented in Section 5. We discuss the results of our study and the star's evolutionary status in Section 6. Some conclusions of the study are summarized in the final section.

2. PARAMETERS OF ι Her

The spectroscopic binary ι Her consists of a bright ($V = 3.80^m$) B3 star and a faint, low-mass companion ($\Delta m = 7.5^m$ [9]). The system's orbital period is $P = 112.825 \pm 0.008$ days [9].

ι Her is in the intermediate region in the HR diagram between β Cep variable stars, which are early B stars, and slowly pulsating B stars of later subtypes [1]. The star's parameters are collected in Table 1, where $T_{\rm eff}$ is the primary's effective temperature, M its mass, g its surface gravity, i the inclination of its rotational axis, $V \sin i$ its rate of rotation, P the system's orbital period, and γ the velocity of the system's center of mass.

The distance between the primary and its low-mass companion is much smaller than $1''$. The contribution of the low-mass (≈ 0.4 $M_\odot$ [9]) companion to the system's combined light is negligible, and we will mean the primary when discussing ι Her.

3. OBSERVATIONS AND REDUCTION OF THE SPECTRA

Our spectroscopy of the ι Her system was acquired as part of our program to search for rapid line-profile variations in the spectra of early-type stars [12]. The observations were made during three nights—May 25, May 29, and June 2, 2004—with

Table 1. Parameters of the ι Her system

Parameter	Value	Reference
$T_{\rm eff}$, K	16 500	[11]
$M/M_\odot$	7−8	[6, 9]
$\log (L/L_\odot)$	3.26	[9]
$\log g$	4.0	[11]
$V \sin i$, km/s	≈ 10	[11]
i, deg	≈ 90	[6]
P, days	112.825 ± 0.008	[9]
γ, km/s	-19.9 ± 0.2	[9]

the BOES optical-fiber echelle spectrograph [13] of the BOAO 1.8 m telescope equipped with a CCD (2048×4096 pixels, 15×15 μm pixel size).

We took 69 echelle spectra with spectral resolution $R \approx 44\,000$ over a wide spectral range: 3782 Å $< \lambda < 9803$ Å. Of these spectra, 14 were acquired during $\approx 2.3^{\rm h}$ on the first night, 10 during $\approx 1^{\rm h}$ on the second night, and 45 during $\approx 5.2^{\rm h}$ on the third night. The total observing time was about $8.5^{\rm h}$. Since the star is rather bright, a short exposure time (about 3−7 min) provided a high signal-to-noise ratio, S/N ≈ 300. The time intervals between subsequent spectra were 6−10 min.

The images were reduced in the standard way using the IRAF package. Subsequent spectral processing was carried out using a version of the Dech package [14] modified in 2004 (Dech20T). To study the line-profile variations, we normalized the spectra to the continuum, which was determined according to the following automated scheme. We used the median filter and other broadband filters in each order of the echelle spectrum to filter out narrow spectral features. Regions containing broad spectral features (such as hydrogen lines) in each order were replaced with interpolated values from adjacent orders where such regions were not present. Finally, the resulting two-dimensional spectrum was smoothed with a two-dimensional moving filter. The image formed in this way is the two-dimensional continuum of the studied spectrum. Further, each individual two-dimensional CCD spectrum was normalized to this continuum.

The continuum-placement technique used here has several advantages compared to the traditional one. The main advantage is the possibility to very accurately reconstuct the physical continuum in regions of broad spectral features. For example, in our study, the uncertainty of the continuum reconstruction in
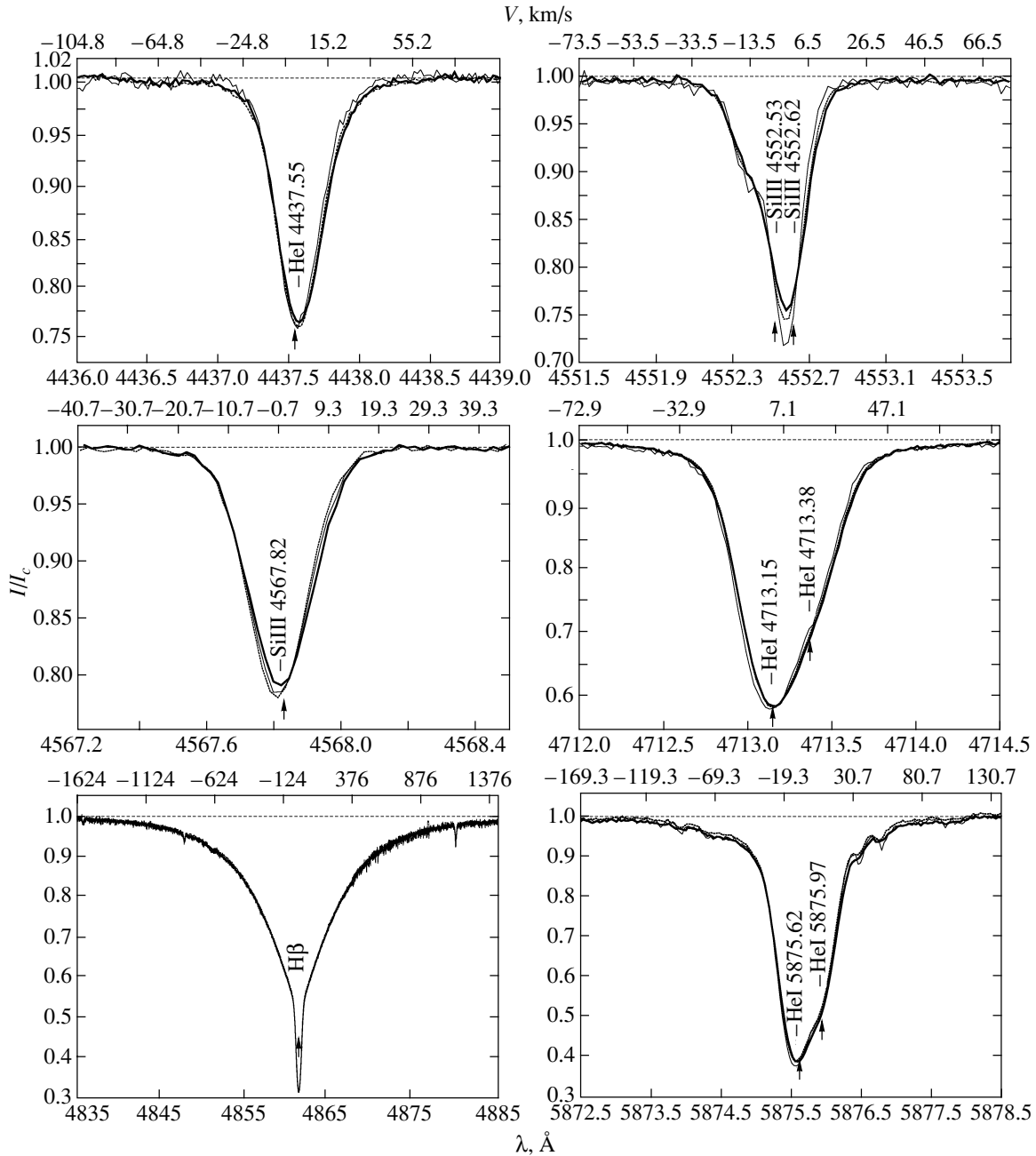
Fig. 1. Mean profiles for the spectra obtained on May 25 (thin solid curve), May 29 (dashed curve), and June 2 (bold solid curve), 2004. The intensities, I, are relative to the continuum intensity, I_c. The vertical arrows correspond to the laboratory line wavelengths.

the regions of the Hα, Hβ, Hγ, and Hδ lines is constant at about 1%.

We tested the continuum-placement technique in a special study of the variability of Balmer line profiles in Ap/Bp stars [15, 16], where we studied differential profile variations in the course of the rotation of the program stars. We investigated the accuracy of the continuum placement via comparisons with model line profiles. When using the same technique

and spectroscopic material of approximately the same quality as in this study, though with a poorer signal-to-noise ratio ($\approx$100 near the Hβ line), the standard deviations of the differential spectra in the region of the hydrogen lines were within 0.2−0.3%.

The wavelengths were converted to the heliocentric scale in the standard way. To facilitate our analysis of the profile variations, we use the mean radial velocity of the center of mass of the ι Her system,

$V_{\text{rad}} = -19,9$ km/s [9] (Table 1), as the zero point of our wavelength scale.

4. LINE PROFILE VARIATIONS

We identified more than 100 lines of H, He, C, N, O and other elements in the resulting spectra. We carried out a detailed analysis for six lines: HeI 4437.551 Å SiIII 4552.616 Å SiIII 4567.82 Å HeI 4713.145, 4713.376 Å Hβ, and HeI 5875.621, 5875.966 Å. These lines were selected based on the following criteria:

(a) the lines were not blended,

(b) the residual intensities at the line centers were $r \leq 0.8$.

The HeI and SiIII lines in our list can be effectively used to search for profile variations due to NRPs [17].

4.1. Variations of the Mean Profiles

To study the profile variations on time scales of days, all the spectra acquired during each of the three observing nights were averaged. Figure 1 displays the resulting mean spectra of the star near the selected HeI, SiIII, and Hβ lines.

We can see from Fig. 1 that the largest variation amplitude for the mean profile occurs near the centers of the studied lines, probably due to the low $V \sin i$ for ι Her. The variability amplitude at the line centers is 0.5−2% in units of the continuum adjacent to the lines.

4.2. Differential Profiles.
A Search for Variable Features

We derived differential profiles (the individual line profiles minus the mean profile) in order to identify variable features in the line profiles in all the available spectra. The line-profile variations are displayed in Fig. 2 in the form of maps of the density of the differential profiles of the studied lines in the spectrum of ι Her for the observations obtained on June 2, 2004. The time T (in hours from the beginning of the observations) increases upwards.

Profile variations detectable by eye are present only near the line center, in the velocity range ± 30 km/s. The absence of appreciable profile variations at higher velocities is probably due to the low amplitude of the profile variations outside a band with width $\pm(V \sin i + W)$, where $W \approx 20$ km/s is the half-width at half-maximum of weak lines in the spectrum.

Note that the variability pattern is very similar for all the differential line profiles. A quasiabsorption feature (plotted black) is visible near the line center at

a velocity of ≈ -10 km/s at the beginning of our observations. With time, this feature first ($T = 0^{\text{h}}-2^{\text{h}}$) move toward negative velocities (to ≈ -20 km/s), then ($T = 2^{\text{h}}-3^{\text{h}}$) moves back toward positive velocities, reaching its highest positive velocity by $T \approx 4^{\text{h}}$, and finally moves to the line center again during $T = 4^{\text{h}}-5.2^{\text{h}}$.

Quasiemission features (plotted in white and gray shades) are located symmetrically about the quasiabsorption features. The movements of the quasiemission features of all the studied profiles are symmetric relative to the movements of their quasiabsorption features. This variability pattern is characteristic of profile variations due to nonradial photospheric pulsations (see, for example, [18, 19]). This suggests that the variability on time scales of several hours are due to NRPs.

5. REGULAR PROFILE VARIATIONS
5.1. Fourier Analysis of the Profile Variations

In order to reveal the mechanism giving rise to the profile variations, we must determine whether the profile variations are regular (cyclic) to some extent, irregular (stochastic), or a superpositions of regular and irregular variations. We carried out a Fourier analysis in order to analyze the variations in detail and to search for periodic components.

We constructed time series $\Delta I(t, \lambda)$ for each of the studied lines—differential intensities for the given profile at time t for wavelength λ. The values of λ were translated into Doppler shifts, V, from the profile center (in the reference frame of the star). For each such time series, we calculated the power-spectrum density of the discrete Fourier transform [20].

We estimated the power-spectrum density of the Fourier transform by calculating the Schuster periodogram [21]:

$$D(\nu, V) = \frac{1}{N^2} \left| \sum_{k=0}^{N-1} \Delta I(t_k, V) e^{-i2\pi\nu t_k} \right|^2. \quad (1)$$

Here, $\{t_k\}$ is the series of times when the analyzed quantity, $\Delta I(t_k, V)$, was measured.

A discrete Fourier power spectrum is the convolution of the actual Fourier spectrum and the spectral window describing the time grid used [21]. For this reason, false peaks can appear in the discrete Fourier spectrum, making it necessary to apply cleaning algorithms. We used the CLEAN algorithm [22] for this purpose, in the modification described in [23].

We applied the CLEAN algorithm to the time series constructed for all possible V values along the profiles of the studied lines, in a strip with width
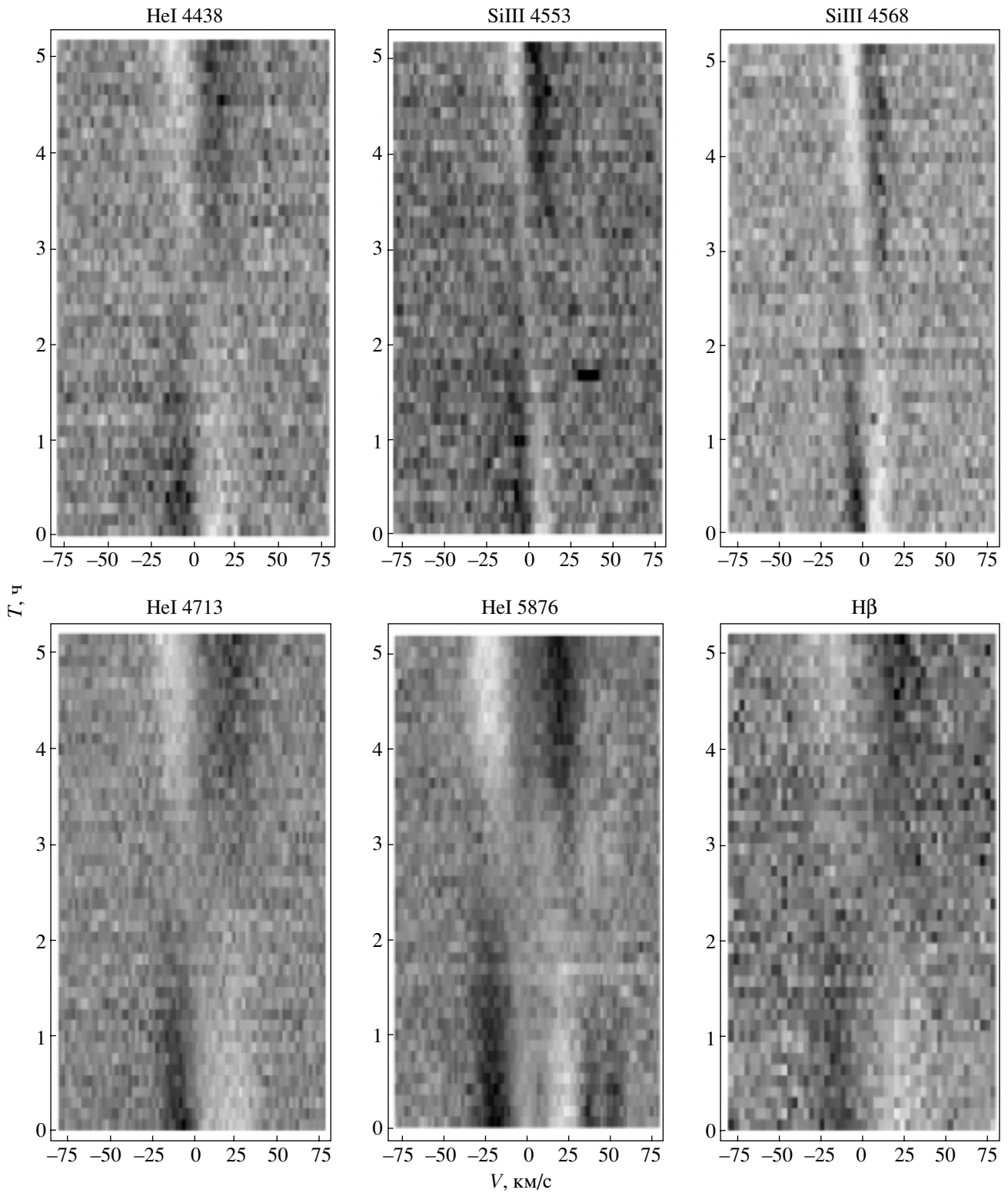
Fig. 2. Dynamical spectra of the line-profile variations in the spectrum of ι Her on June 2, 2004. Deviations of the individual line profiles from the mean are plotted as different shades of gray. Light and dark regions in the diagrams correspond to parts of the profile that are above or below the mean profile level. The time interval between subsequent spectra was 7 min. Time increases upwards.
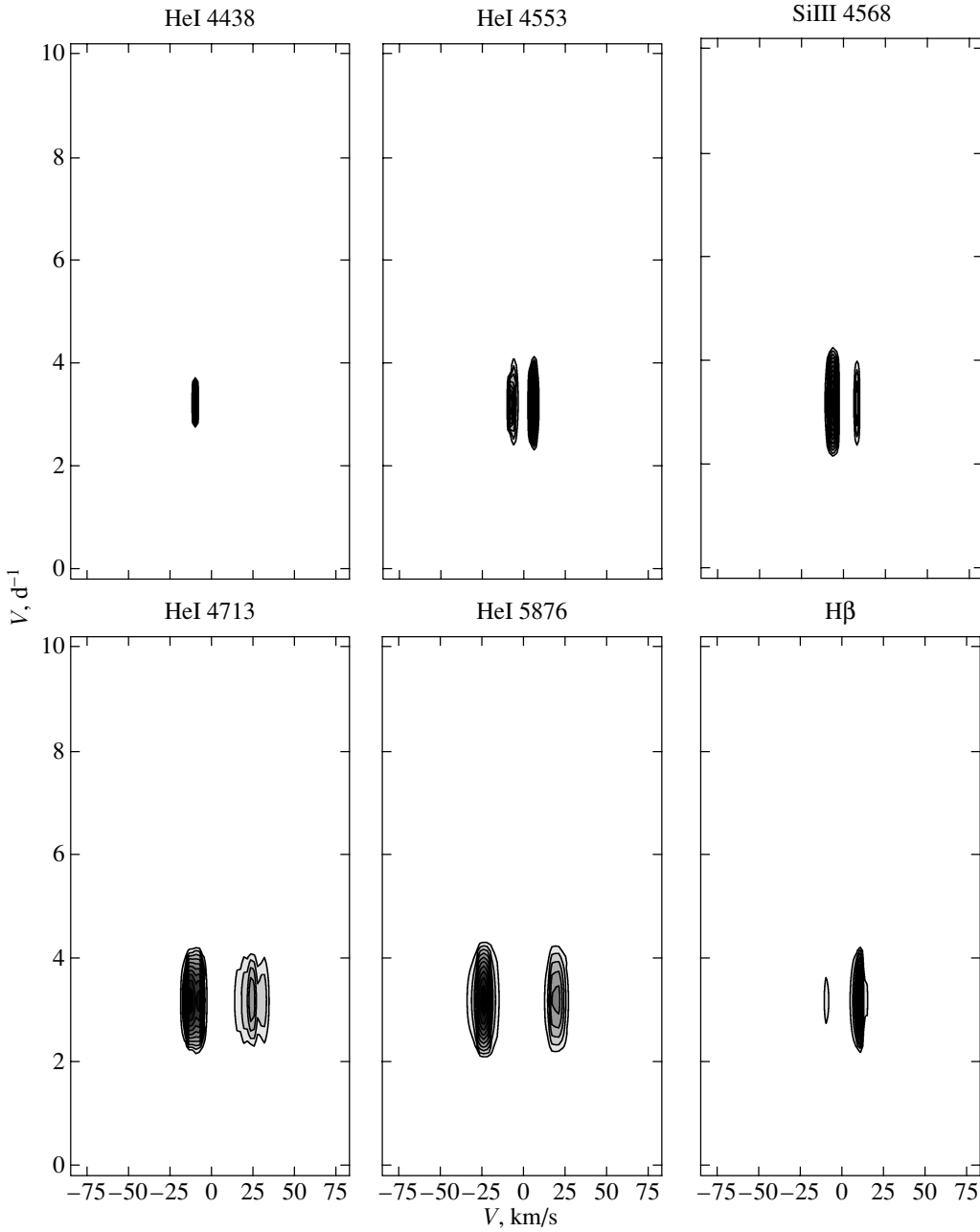
Fig. 3. Fourier spectra of variations of the differential line profiles after cleaning the Fourier power spectrum for the observations of June 2, 2004 using the CLEAN algorithm in the frequency range $\nu = 0-10\,\mathrm{d}^{-1}$. The diagram shows only those amplitudes of the Fourier spectra corresponding to significance levels $q \geq 10^{-7}$ for the hypothesis that a strong peak in the white-noise periodogram is significant are shown. The darker places of the diagrams correspond to larger amplitudes.

± 80 km/s. To smooth the noise component of the profile variations, we averaged the values of ΔI in a spectral window with width $\sigma = 2-5$ pixels ($\approx 0.06-0.15$ Å). The choice of different values of σ turned out to have virtually no influence on the resulting Fourier spectrum.

When analyzing Fourier spectra, the significance levels for various periodogram peaks are of utmost importance if we wish to clarify which peaks correspond to real periodic components of the line-profile-variation time series, $\Delta I(t, V)$. We applied the relation from [20, 23] for the probability for a value of a normalized white-noise periodogram, $Z = D(\nu, V)/(\sigma_0^2/N)$, to exceed a given value z:

$$F(z) = P(Z > z) = 1 - \left(1 - e^{-z}\right)^{1/N_i}, \quad (2)$$

where σ_0^2 is the dispersion of the white-noise readings and N_i is the number of independent readings of the periodogram. Specifying a small value,

HeI 4438   SiIII 4553   SiIII 4568

HeI 4713   Hβ   HeI 5876
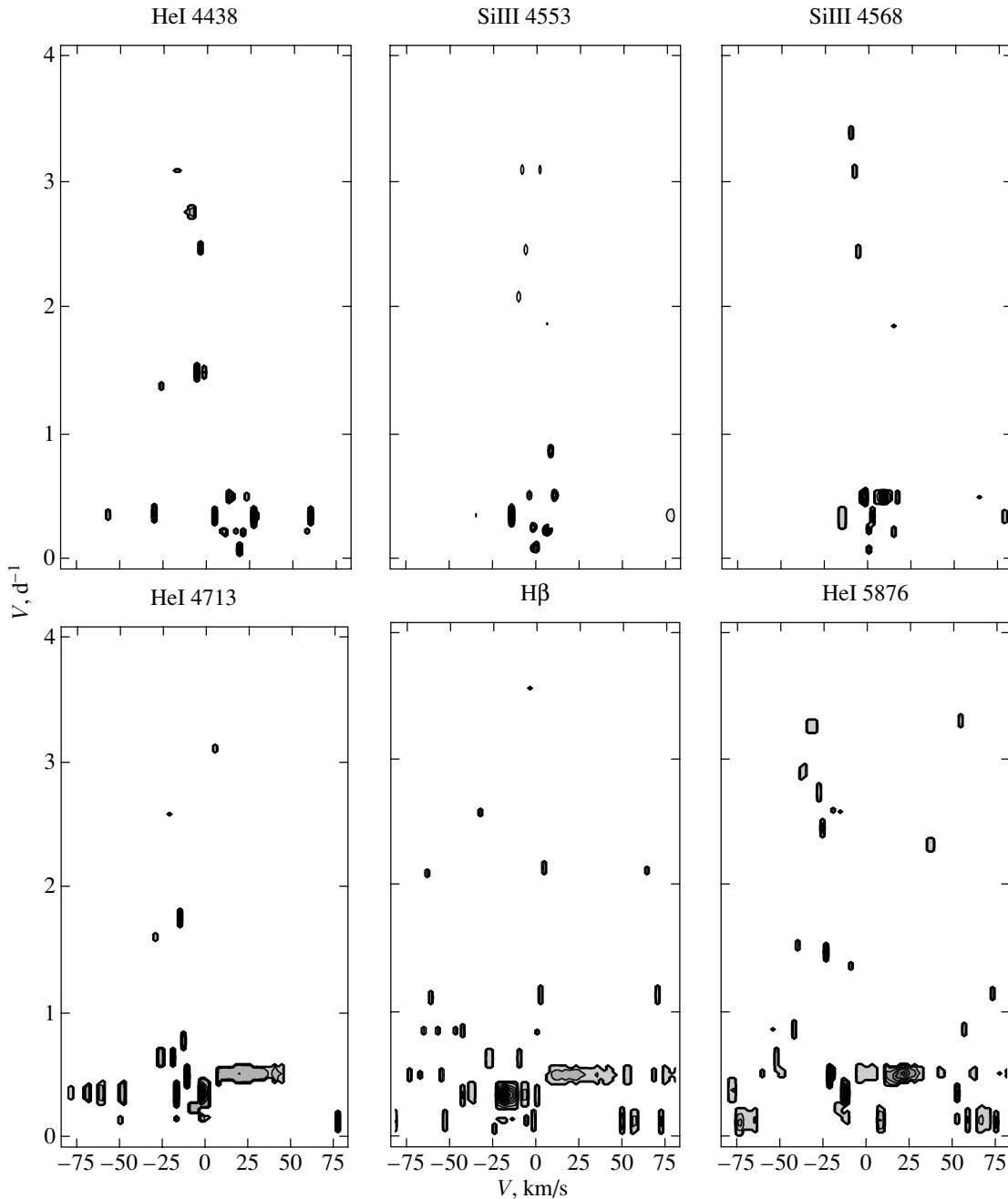
V, km/s

Fig. 4. Same as Fig. 3 for all the observations acquired on May 25, May 29, and June 2, 2004. In contrast to Fig. 3, Fourier-spectrum amplitudes corresponding to significance levels $q \geq 10^{-3}$ are presented.

$q = F(Z_q) \ll 1$, we have:

$$Z_q = -\ln\left[1 - (1-q)\right]^{1/N_i} \approx \ln(N_i/q). \quad (3)$$

When using the CLEAN technique to identify peaks of the periodogram that are significant at a level q, we considered only peaks with heights in the initial periodogram exceeding Z_q. The value of Z_q depends on the choice of N_i. The usual choice for evenly spaced series is $N_i = N/2$ [20]. It is suggested in [24] to use an empirical relation that gives much

larger values of N_i (by a factor of two or three) for unevenly spaced series.

The authors of [25] claim that the results of [24] are erroneous, and suggest the use of the classical value, $N_i = N/2$. Note that, according to (3), the dependence of Z_q on N_i is logarithmic, and variations of N_i within a factor of two or three change Z_i by within 20%. With this in mind, we will use the value $N_i = N/2$ in our subsequent identifications of significant peaks in the line-profile-variation peri-

Table 2. Frequencies ν and periods P for periodic harmonics of the line-profile variations in the spectrum of ι Her

No.	ν, d^{-1}	σ	P	HeI 4438	SiIII 4553	SiIII 4568	HeI 4713	Hβ	HeI 5876	Status
1	0.12 ± 0.14	0.03	8.3^{d}	+	+	+	+	+	+	:
2	0.34 ± 0.14	0.08	2.9^{d}	+	+	+	+	+	+	+
3	0.49 ± 0.14	0.12	2.0^{d}	+	+	+	+	+	+	:
4	0.82 ± 0.14	0.20	1.3^{d}	−	+	−	−	+	+	+
5	1.1 ± 0.14	0.26	21.8^{h}	−	−	−	+	+	+	+
6	1.45 ± 0.14	0.35	16.6^{h}	+	−	−	−	−	+	:
7	1.8 ± 0.14	0.43	13.3^{h}	−	+	+	+	−	−	+
8	2.1 ± 0.14	0.51	11.4^{h}	−	+	−	−	+	−	:
9	2.4 ± 0.14	0.58	9.2^{h}	+	+	+	−	−	+	+
10	2.8 ± 0.14	0.68	8.6^{h}	+	−	−	−	−	+	+
11	3.1 ± 0.14	0.75	7.7^{h}	+	+	+	+	−	−	+
12	3.4 ± 0.14	0.82	7.1^{h}	−	−	+	−	+	+	+

Note: In the third column, σ is the dimensionless pulsation frequency (cf. Subsection 6.6.3).
The symbol "+" in a column of a particular line means that a component of the indicated frequency is present in the periodogram.
The symbol "+" in the last column means that the component of the indicated frequency is probably real, whereas the symbol ":" means that the harmonic may correspond to a false peak in the periodogram.

odogram. The statistical properties of white-noise periodograms for significantly unevenly spaced series are complex and poorly studied [20], and we will use the value $q \leq 10^{-3}$, which is lower than the usual value $q \leq 10^{-2}$, to help ensure more reliable identification of significant periodogram peaks.

5.2. Fourier Analysis
of the Observations of June 2, 2004

We performed our Fourier analysis of the line profiles and plotted the periodograms in two stages. In the first stage, we analyzed the observations for the last night, June 2, 2004. In the second stage, we analyzed all the observations together.

Figure 3 is a contour diagram of the densities of the Schuster periodogram after cleaning the Fourier density spectrum using the CLEAN algorithm for all the studied lines in the spectrum of ι Her, based on 45 line profiles in the spectra taken on June 2, 2004 during a time $T_{\mathrm{June\,2}} = 5.2^{\mathrm{h}}$.

For avoid clutter in the presentation, the contour diagrams were plotted after removing all periodogram values corresponding to significance levels $q \leq 10^{-7}$ for the hypothesis that a strong peak in the white-noise periodogram is significant. Thus, only periodogram components that were significant at this level were retained in the diagrams.

All the spectra possess a broad peak in the density of the Fourier power spectrum at the frequency $\nu \approx 3.1 \, \mathrm{d}^{-1}$. Note that the periodogram maxima coincide for all the studied lines, and are near the $\pm V \sin i$ strip, providing further evidence that the line-profile variations in the spectrum of ι Her are due to NRPs.

The quantity $T = 1/\nu \approx 7.7$ hours exceeds the total duration of the observations on June 2, 2004. The resolution of the Fourier spectrum is $\approx 1/T_{\mathrm{observ}} \approx 4.6 \, \mathrm{d}^{-1}$ [23], where $T_{\mathrm{observ}} = T_{\mathrm{June\,2}}$ is the total duration of the analyzed observations; this value is larger than ν. Thus, our analysis of the Fourier spectra of the line profile variations of ι Her on June 2, 2004 does not enable us to draw conclusions about the presence of a periodic component with the frequency $\nu \approx 3.1 \, \mathrm{d}^{-1}$. We can only assert that the profile variations for all the studied spectral lines on June 2, 2004 are nearly sine-shaped, with a period about 7–8 hours. To determine if the periodic component with $\nu \approx 3.1 \, \mathrm{d}^{-1}$ is real, we must jointly analyze all our observations of ι Her.

5.3. Fourier Analysis of All the Observations

We analyzed the observations of May 25 and 29, 2004 together with the observations of June 2, 2004. When computing the Fourier spectra of the line-profile variations, we used differential profiles derived

by subtracting the mean profile based on all three observing lights from the individual line profiles.

Since the gaps in the time series were large, we used the CLEAN algorithm to remove false peaks. The computations assumed a significance level $q = 10^{-3}$ for the hypothesis that a strong peak is present in the white-noise periodogram.

Several dozen individual peaks are present in the computed periodograms. However, components significant at the $q = 10^{-3}$ level were found only at frequencies $\nu = 0-4\,\mathrm{d}^{-1}$. All the periodogram peaks that are significant at this level exceed the Z_q values computed using (3) by a factor of two or more, providing additional confirmation that they are real.

Periodograms of the Fourier power spectrum for the profile variations for all the lines studied in the above range are shown in Fig. 4. The frequencies of detected harmonic components are collected in Table 2. Only those components of the Fourier-transform power spectrum that are present for the profiles of *at least two lines* are presented in this table. According to [23, 26], the uncertainties of the frequencies in Table 2 are $\approx 1/T_{\mathrm{observ}}$, where $T_{\mathrm{observ}} = 7.24$ d is the total duration of the observations.

6. DISCUSSION OF THE RESULTS

6.1. Profile Variations with Periods Exceeding 7^h

Let us consider, one by one, the harmonic components of the line profile variations we detected and compare our results with those of other studies. The period $P_1 = 8.3$ d could be related to the star's rotational period. Using the data in Table 1, we can estimate an upper limit for the star's rotational period: $P_{\mathrm{rot}} \leq 2\pi R_*/V \sin i \approx 24$ days, consistent with the possibility that P_1 is associated with the rotation period. The star's radius, $R_* \approx 4.7\,R_\odot$, was determined from the values of M and $\log g$ in Table 1. This value essentially coincides with the standard value for B3 main-sequence stars, $R_* \approx 4.8\,R_\odot$ [27]. P_1 is longer than the total duration of our observations (7.25 days), and additional observations with a longer time span are needed to confirm its reality.

The component ν_2 corresponds to the main low-frequency component detected in [9], $\nu = 0.28671\,\mathrm{d}^{-1}$, within the errors. The component ν_3 is close to $0.5\,\mathrm{d}^{-1}$, and so may be the first harmonic of the one-day period, and longer observations are required to confirm if it is real. The component ν_4 corresponds within the errors to the $0.77\,\mathrm{d}^{-1}$ harmonic detected by Chapellier et al [9] in their analysis of the radial velocities of UV lines determined in [28].

The component ν_6 appears in the computed periodograms for only two lines, and spectroscopic observations of ι Her with shorter gaps are needed to confirm the reality of this component. The component ν_7 appears in the profile variations of the SiIII 4553 Å, SiIII 4568 Å, and HeI 4713 Å lines. Within the uncertainties, it coincides with the $1.72\,\mathrm{d}^{-1}$ component detected in the radial-velocity analysis for the SiII 4131 Å doublet [29]. The frequency difference for the components ν_8 and ν_7, $0.3\,\mathrm{d}^{-1}$, is close to the frequency of component ν_2; in addition, ν_8 was detected for only two lines. Thus, we cannot exclude the possibility that ν_8 is an alias of ν_7.

The frequency of the component ν_9 coincides within errors with the frequency $\nu = 2.42\,\mathrm{d}^{-1}$ detected, like in the case of ν_6, in the radial-velocity analysis for the SiII 4131 Å doublet [29]. None of the components $\nu_{10}-\nu_{12}$ were detected in earlier studies of the ι Her system. Nevertheless, they stand out quite clearly in the power spectrum of the Fourier transform (Fig. 4), and their positions coincide with the position of a broad peak in the periodogram of profile variations of all the studied lines from the observations of June 2, 2004 (Fig. 3).

The symbol "+" in the last column of Table 2 marks frequencies that, in our opinion, are genuinely present in the Fourier spectrum of the line-profile variations. The symbol ":" indicates that the reality of that frequency in the Fourier spectrum requires additional verification.

Thus, our analysis of the Fourier spectrum of the line-profile variations in the spectrum of ι Her revealed eight harmonic components at frequencies $0.3\,\mathrm{d}^{-1} \leq \nu \leq 3.4\,\mathrm{d}^{-1}$ with periods from 7.1^h to 2.9^d. The possible presence of four additional Fourier-spectrum components in the range $0.12\,\mathrm{d}^{-1} \leq \nu \leq 2.1\,\mathrm{d}^{-1}$ should be studied further.

6.2. Short-Period Profile Variations

Many studies of ι Her have indicated photometric and radial-velocity variations with periods $P \leq 6^h$, corresponding to the frequencies $\nu = 4-34\,\mathrm{d}^{-1}$ [7–9].

Our Fourier analysis of the profile variations demonstrated an *absence* of any significant (at the $q \leq 10^{-2}$ level) components of the Fourier spectrum in this frequency range, for the analysis both of the June 2, 2004 observations alone and for all our observations of ι Her.

Only when using the significance level $q = 0.05$ for the hypothesis that a strong peak in the white-noise periodogram is real were we able to reveal a number of weak components in the Fourier spectrum, with

frequencies $\nu = 5.8, 8.3, 8.6, 8.9$, and $9.8 \, \mathrm{d}^{-1}$. All the detected Fourier components, except for $\nu = 8.9 \, \mathrm{d}^{-1}$, were found in the Fourier spectrum for only one line, and were observed outside the $\pm(V \sin i + W)$ strip, so we consider them to be false peaks due to chance outliers in the periodogram of the noise component of the signal.

The $8.9 \, \mathrm{d}^{-1}$ component was found in the Fourier spectra of the profile variations for two lines, HeI 4438 Å and SiII 4553 Å, within the $\pm V \sin i$ strip, and may be real, though the absence of this peak in the Fourier power spectra of the profile variations derived solely from the June 2, 2004 observations provides evidence against this possibility.

We conclude that the detections of rapid spectral or photometric variations in several earlier studies resulted either from errors in the procedures used to analyze those time series or from a transient character for such short-period variations of ι Her. Note also that the above frequencies for the short-period profile variations are outside all regions of pulsational instability for B3 stars [2].

In order to resolve the question of whether or not there are real rapid profile variations in the spectrum of ι Her, we are planning to carry out spectroscopic observations of ι Her during two to four complete nights in a row, which will enable us to significantly improve our identification of the frequencies of the detected components, and possibly to find new harmonics.

6.3. Evolutionary Status of ι Her

It has been suggested in many studies that ι Her possesses spectral characteristics typical of both SPB stars and the hotter β Cep stars [6, 7, 29]. The position of ι Her in the upper part of the region occupied by SPB stars in the HR-diagram [30] is consistent with this assertion.

At the same time, our analysis shows that all the detected profile-variation frequencies are within the range of frequencies for the pulsational instability of SPB stars [30, 31], whereas the short-period profile variations characteristic of β Cep stars are not present.

In order to investigate the evolutionary status of ι Her, let us compare our derived frequencies for the regular line-profile variability in the spectrum of ι Her with the results of computations of pulsational instability of stars in the upper main sequence [32]. In [32], evolutionary tracks were computed for stellar masses of $1.5 \leq M/M_\odot \leq 40$ and normal chemical composition ($X = 0.70$, $Z = 0.02$), in the interval of ages between the zero-age main sequence (ZAMS) and the depletion of hydrogen in the core. The parameters of nonadiabatic stellar pulsations with the range

of dimensionless frequencies $0.05 \leq \sigma \leq 6$ were computed for all these ages, where, according to [32],

$$\sigma = \frac{\sqrt{\pi}\nu}{\sqrt{G\overline{\rho}}} = 0.067 \left(\frac{R}{R_\odot}\right)^{3/2} \left(\frac{M}{M_\odot}\right)^{-1/2}. \quad (4)$$

Here, G is the gravitational constant, $\overline{\rho}$ the star's mean density, and R and M its mass and radius, respectively. The numerical value of the coefficient in (4) was computed for frequencies ν expressed in d^{-1}.

We used (4) and the star's parameters in Table 1 to calculate the dimensionless frequencies, σ, for all the detected frequencies of the harmonic components of the line-profile variations in the spectrum of ι Her, given in the third column of Table 2. If we exclude from the harmonic-component frequencies in this table those that we consider to be doubtful in any sense, the remaining frequencies are $\sigma \in [0.06-0.85]$.

Since ι Her is close to the strip in the HR diagram occupied by stars in the stage of core hydrogen depletion [30], we plotted these frequencies on a $\log T_{\mathrm{eff}}-\sigma$ diagram for stars with bolometric luminosities corresponding to absolute magnitudes $0.5^m-1.0^m$ higher than those for ZAMS stars by [32]. The slanted shading in the diagrams of Fig. 5 indicates the SPB-star instability region, which is related to high g modes of NRPs. The points in the upper left-hand side of the diagrams correspond to the dimensionless frequencies for the pulsational instability of β Cep stars, which are probably related to p modes.

The numbers in the diagrams' upper right corners are spherical harmonic degrees of the pulsation modes. It follows from Fig. 5 that SPB stars are stable against pure radial oscillations ($l = 0$), and that dipole and quadrupole oscillations ($l = 1, 2$) are possible only in a very narrow interval of the dimensionless frequencies, $\sigma \approx 0.2$.

Comparing our derived set of frequencies for the harmonic components of the profile variations (the filled rectangle in Fig. 5) to the region of pulsation instability for SPB stars, we see that the values $l = 4-8$ are most probable.

The displacement and velocity of an elementary photospheric volume of a nonradially pulsating star with spherical coordinates (θ, ϕ) are proportional to the spherical harmonics, $Y_{l,m}(\theta, \phi)$ [18]. The following relations are use to determine the order of the spherical harmonic, l, of the pulsation modes and the azimuthal parameter, m, for upper-ZAMS stars [19]:

$$l \approx 0.076 + 1.110 \frac{\Delta\Phi_0}{\pi}, \quad (5)$$

$$m \approx -1.028 + 0.613 \frac{\Delta\Phi_1}{\pi},$$

where $\Delta\Phi_0$ is the total variation of the phase, Φ_0, for the studied periodic component of the line-profile
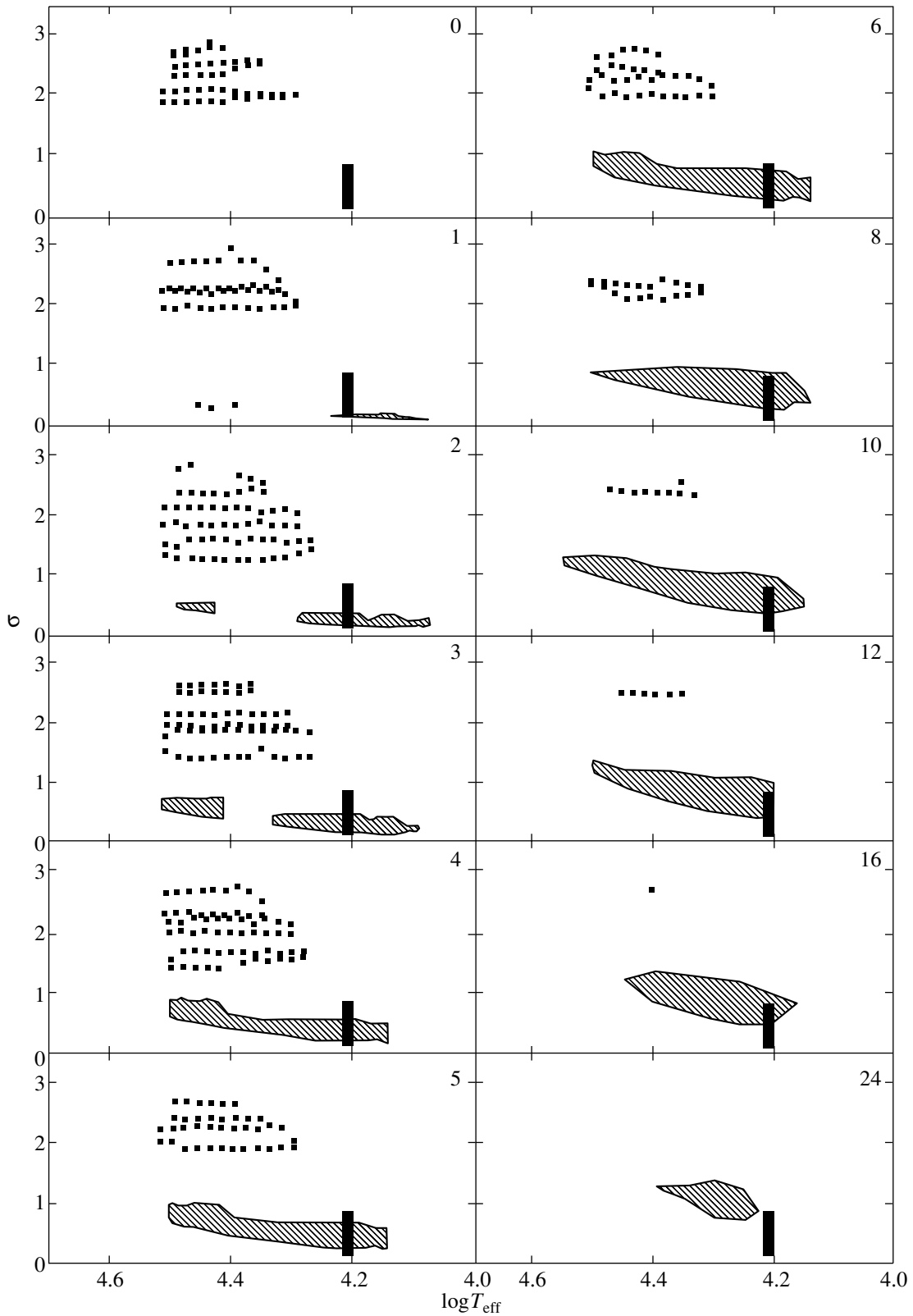
Fig. 5. Position of the frequency set for the line profile variations in the spectrum of ι Her (the filled rectangle) in the $\log T_{\mathrm{eff}}-\sigma$ diagram for upper-MS stars with bolometric luminosities corresponding to absolute magnitudes higher than those for ZAMS stars by $0.5^{m}-1.0^{m}$ [32]. The spherical harmonic degrees of the pulsation modes are indicated in the upper right-hand corners of each diagram. The domain of pulsation frequencys of SPB stars is shaded. The points in the upper left side of the diagrams correspond to the pulsation frequencies of β Cep stars.

variations along the line profile in the $\pm V \sin i$ strip and $\Delta\Phi_1$ is the same value for the first harmonic.

Unfortunately, the low $V \sin i$ for ι Her hindered our attempts to derive accurate l and m values for the spherical harmonics using this method. The phase Φ_0 in the $\pm V \sin i$ strip experiences a jump, $\Delta\Phi_0$, of at least 2π, suggesting only values $l \geq 2$ are possible, in agreement with our earlier conclusion that $l = 4-8$.

7. CONCLUSIONS

We have investigated variations of the line profiles in the spectrum of the bright B3IV star ι Her with high time and spectral resolutions. Our observations and analysis enabled us to draw the following conclusions.

(1) All the studied lines with $r_{max} < 0.8$ have variable profiles. The variability amplitude is $0.5-2\%$, in units of the flux in the adjacent continuum.

(2) The central parts of the profiles of all the studied lines in the spectrum of ι Her revealed regular profile variations with frequencies in the range $\nu = 0.3-3.4 \, \mathrm{d}^{-1}$, or with time scales $7^{\mathrm{h}}-2.9^{\mathrm{d}}$. These variations can be interpreted as g modes of nonradial pulsations with spherical-harmonic orders $l = 4-8$.

(3) We find no evidence for the high-frequency harmonics, $\nu \geq 4 \, \mathrm{d}^{-1}$, that were reported in earlier studies. We conclude that ι Her is a slowly pulsating B star.

REFERENCES

1. C. Waelkens, Astron. Astrophys. **305**, 887 (1991).
2. A. A. Pamyatnykh, Acta Astron. **49**, 189 (1999).
3. D. L. Edwards, Mon. Not. R. Astron. Soc. **97**, 99 (1937).
4. K. Kodaira, Publ. Astron. Soc. Jpn. **23**, 129 (1971).
5. H. A. Abt and S. G. Levy, Astrophys. J., Suppl. Ser. **36**, 241 (1978).
6. M. A. Smith, Astrophys. J. **224**, 927 (1978).
7. M. A. Smith, Astrophys. J. **246**, 905 (1981).
8. E. Chapellier, J.-M. Le Contel, J.-C. Valtier, *et al.*, Astron. Astrophys. **176**, 255 (1987).
9. E. Chapellier, P. Mathias, J.-M. Le Contel, *et al.*, Astron. Astrophys. **362**, 189 (2000).
10. *The Hipparcos and Tycho Catalogues*, ESA SP-1200 (ESA, Noordwijk, 1997).
11. O. I. Pintado and S. I. Adelman, Mon. Not. R. Astron. Soc. **264**, 63 (1993).
12. A. F. Kholtygin, D. N. Monin, A. E. Surkov, and S. N. Fabrika, Pis'ma Astron. Zh. **29**, 208 (2003) [Astron. Lett. **29**, 175 (2003)].
13. http://www.boao.re.kr/BOES/BOESppt3.files/frame.htm.
14. G. A. Galazutdinov, Preprint No. 92 SAO (Special Astrophysical Observatory, Crimea, 1992).
15. G. Valyavin, O. Kochukhov, D. Shulyak, *et al.*, in *Proceedings of the East Asian Meeting of Astronomy, Korea, 2005* (in press).
16. D. Shulyak, G. Valyavin, and B.-C. Lee, Astron. Astrophys. (2005) (in press).
17. Th. Rivinius, D. Baade, and S. Stefl, Astron. Astrophys. **411**, 229 (2003).
18. J. H. Telting and C. Schrijvers, Astron. Astrophys., Suppl. Ser. **121**, 343 (1997).
19. J. H. Telting and C. Schrijvers, Astron. Astrophys. **317**, 723 (1997).
20. D. S. Scargle, Astrophys. J. **263**, 835 (1982).
21. V. V. Vityazev, *Spectral−Correlation Analysis of Uniform Time Series* (S.-Peterburg. Gos. Univ., St. Petersburg, 2001) [in Russian].
22. D. H. Roberts, J. Lehar, and J. W. Dreher, Astron. J. **93**, 968 (1987).
23. V. V. Vityazev, *Analysis of Nonuniform Time Series* (S.-Peterburg. Gos. Univ., St. Petersburg, 2001) [in Russian].
24. J. H. Horne and S. L. Baliunas, Astrophys. J. **302**, 757 (1986).
25. I. Antokhin, J.-F. Bertrand, R. Lamontange, and A. F. J. Moffat, Astron. J. **109**, 817 (1995).
26. V. V. Vityazev, Astron. Astrophys. Trans. **21**, 1 (2002).
27. *Allen's Astrophysical Quantities*, 4th ed., Ed. by A. N. Cox (AIP Press, Springer, New York, 2000).
28. J. B. Rogerson, Jr., Astron. J. **89**, 1876 (1984).
29. P. Mathias and C. Waelkens, Astron. and Astrophys. **300**, 200 (1995).
30. W. A. Dziembowski, P. Moskalik, and A. A. Pamyatnykh, Mon. Not. R. Astron. Soc. **265**, 588 (1995).
31. W. A. Dziembowski, Astron. Soc. Pac. Conf. Ser. **78**, 275 (1995).
32. L. A. Balona and W. A. Dziembowski, Astron. Astrophys. **309**, 221 (1999).

Translated by N. Samus'